Eur Biophys J (1995) 24: 77–84

European Biophysics Journal

The subdomain structure of human serum albumin in solution under different pH conditions studied by small angle X-ray scattering

Johnny R. Olivieri[1], **Aldo F. Craievich**[2]

[1] Departamento de Física, UNESP, CP 136, São José do Rio Preto-SP, CEP 15054-000, Brazil
(e-mail: johnny@minerva.ibilce.unesp.br, Fax: +55-172-248692)
[2] Laboratório Nacional de Luz Síncrotron, Campinas – SP, and Instituto de Física, USP São Paulo, SP-Brazil

Received: 28 March 1994 / Accepted in revised form: 10 January 1995

Abstract. Small-angle X-ray scattering (SAXS) was used to study structural characteristics of human serum albumin (HSA) in solution under different pH conditions. Guinier analysis of SAXS results yielded values of the molecular radius of gyration ranging from 26.7 Å to 34.5 Å for pH varying from 2.5 to 7.0. This suggests the existence of significant differences in the overall shape of the molecule at different pH. Molecular models based on subdomains with different spatial configurations were proposed. The distance distribution functions associated with these models were calculated and compared with those determined from the experimental SAXS intensity functions. The conclusion of this SAXS study is that the arrangement of molecular subdomains is clearly pH dependent; the molecule adopting more or less compact configuration for different pH conditions. The conclusions of this systematic study on the modification in molecular shape of HSA as a response to pH changes is consistent with those of previous investigations performed for particular pH conditions.

Key words: SAXS – Human serum albumin – Molecular configuration

1. Introduction

Human serum albumin (HSA), the major component in blood plasma has been the subject of a large number of biochemical and biophysical studies. The importance of HSA stems from the fact that it is involved in bioregulatory and transport phenomena such as the control of osmotic pressure in blood, the transport and storage of fatty acids, amino acids, various metal ions, steroids and other ligands (Peters 1985; Kragh-Hansen 1981).

HSA consists of 585 aminoacids with a molecular weight of 66.5 kD, stabilized by 17 disulphide bridges and contains a single free sulphydryl. HSA and Bovine Serum Albumin (BSA) display approximately 76% sequence homology and the repeating pattern of disulphides are strictly conserved (Behrens et al. 1975; Meloun et al. 1975; Brown 1977). The structure of HSA is organized in a series of nine loops (Fig. 1). These loops repeat in a triplet fashion of large-small-large loops and can be further grouped into three homologous domains of three loops each. The homology of the loops suggests that albumin evolved from a precursor one-third or even one-ninth the present size by gene duplication (MacLachlan and Walker 1977). All but the first of the nine are double loops, based upon a repeating cys-cys pattern which occurs eight times. This permits the division of the molecule into three major *domains* (I, II and III) each of which can be further subdivided into *subdomains* (A and B). The locations of the disulphide bridges appears to confer some rigidity within each subdomain, but the lack of interdomain disulphide bridges allows significant modifications in the shape of HSA in response to changes in pH.

A host of studies of BSA in solution, utilizing various techniques such as sedimentation, dielectric dispersion (Squire et al. 1968), small-angle X-ray scattering (SAXS) (Anderegg et al. 1955; Luzzati et al. 1961; Laggner et al. 1971), hydrodynamic and SAXS (Bloomfield 1966), and small-angle neutron scattering (SANS) (Bendedouch et al. 1983), have led to very different models for the overall shape of albumin with little correlation between them. The above studies indicated that the shape of BSA could be approximated by a prolate ellipsoid, an oblate ellipsoid, a flat prism, a right prism or, three spheres arranged in a row (Table 1). Recent crystallographic results, (Carter et al. 1989, 1990; He and Carter 1992; Ho et al. 1993) have shown that, between pH 5.5 and 7.2, the domains and subdomains are arranged to roughly approximate a triangle or can be referred to as "heart-shaped".

Different forms of serum albumin, denoted E (extended), F (fast), N (normal), B (basic) and A (aged) were encountered and the transitions between them were shown to occur at pH values of 2.7, 4.3, 8.0, 10.0, respectively (Foster 1977). The α-helical content proposed was:

Correspondence to: J. R. Olivieri

E-35%, F-45%, N-55%, B-48% and A-40%. Below pH 4.0, the albumin molecule partially unfolds and expands owing to mutual repulsion of the subdomains, resulting in an increase in its intrinsic viscosity (Foster 1977).

This work aims at a comparative characterization of the molecular shape of HSA at different pH conditions. We used for this investigation the SAXS technique which provides information on the structural characteristics of macromolecules in solution at a superatomic scale. One of the procedures to obtain structural information from SAXS results is based on the comparison of structure functions of proposed models with different configurations of subdomains with those determined from experiments. Even through this technique cannot guarantee the uniqueness of the model, it is widely used and was demonstrated to yield useful information on the structure and on structural variations of a number of macromolecules of biological interest (Glatter 1982).

The known Guinier analysis of SAXS intensity provides a structural parameter, the radius of gyration of the molecule in solution, which is independent of any priori a model. The SAXS method also yields information on the spatial configuration of the molecular subdomains but ignores internal structural details and dynamic features such as, for example, vibration, rotation or internal conformational changes.

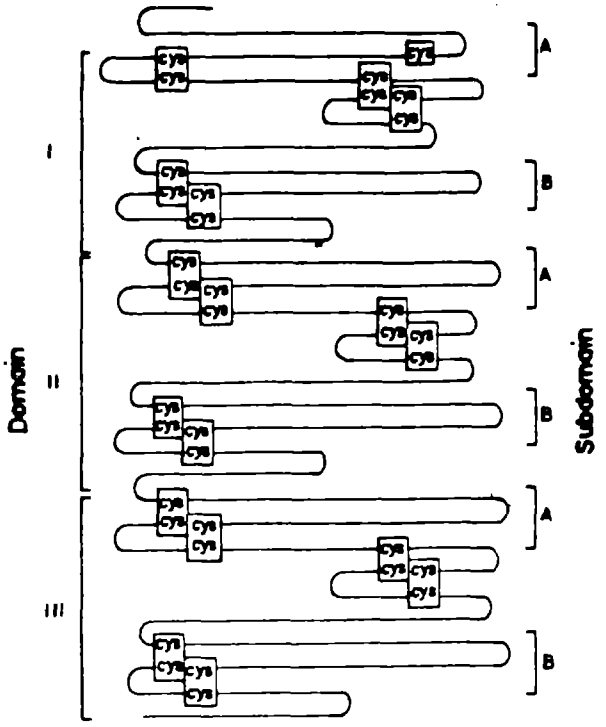

Fig. 1. Schematic representation of the sequence of HSA (Peters 1985) divided into three domains (I, II and III); each domain is further subdivided into subdomains (A and B). The boxed disulphide bridges are strictly conserved between human, bovine, rat and porcine serum albumins

2. Materials, experimental techniques and data analysis procedures

Commercial preparations of HSA defatted and free of globins and other ligands were used for this study. The lyophylized samples were diluted in 0.1 M ammonium formate buffer at the differents pH values of 2.5, 3.0, 3.5, 4.0, 4.5, 5.0 and 7.0.

A Rigaku generator utilizing a Cu X-ray anode operating at 2.5 kW was used for SAXS experiments. The X-ray beam was monochromatized by using a Ni filter and collimated with a block slit system (Kratky 1982). The scattered intensity was measured using a TEC gas position sensitive detector controlled by a microprocessor. The data were analyzed on a Sun Sparc-330 (SUN) computer.

The SAXS measurements were performed within an angular range defined by $0.014\ \text{Å}^{-1} < h < 0.310\ \text{Å}^{-1}$ where $h = \frac{4\pi \sin\theta}{\lambda}$, 2θ being the angle between the incident

Table 1

Techniques	Protein	pH	R_g(Å)	Dimension	Form
Sedimentation and others[a]	BSA	5.2		140×40 Å	Prolate ellipsoid
Hydrodynamics[b]	BSA	3.6			Three spheres in a row
SAXS[c]	PSA	7.0–5.1	32	0.66:1:2	Prolate ellipsoid
		3.7	38	0.25:1:1	Flat prism
SAXS[d]	BSA	4.6	29.8	106×21.5×50 Å	Right prism
				82.5×27.5×63 Å	Rectangular parallelepiped
SAXS[e]	BSA	5.3	30.6		Ellipsoid of revolution
		3.6	27.2		Ellipsoid of revolution
SANS[f]	BSA	5.1	30.5	70×20 Å	Prolate ellipsoid

BSA – Bovine serum albumin
PSA – Porcine serum albumin
[a] Squire et al. 1968
[b] Bloomfield 1966
[c] Laggner et al. 1971
[d] Anderegg et al. 1955
[e] Luzzati et al. 1961
[f] Bendedouch et al. 1983

and scattered X-ray beam and λ the X-ray wavelength. The contributions to the scattering intensity from the solvent, capillary and air were subtracted from the total intensity.

The SAXS measurements were carried out using HSA concentrations between 5 mg/ml and 50 mg/ml. Depending on the protein concentration, typical counting times varied between 5 and 6 h. The maximum count number was of the order of 4.5×10^4 at the lowest scattering angles. All measurements were performed at room temperature (20 °C). The scattering intensities corresponding to HSA at different concentrations and constant pH were extrapolated to zero concentration for each h value. This procedure was used to eliminate the effects of interference between the scattering amplitude produced by each molecule. The extrapolated values yield the experimental scattering intensity function, J(h), for "infinite" dilution. The extrapolated experimental SAXS intensity functions, J(h), were desmeared to suppress the influence from the slit collimation system yielding the corrected intensities, I(h).

A structural parameter related to the overall size and shape of the macromolecule, the radius of gyration R_g, was determined by using the Guinier equation (Guinier and Fournet 1955):

$$I(h) = I(0) \exp\left[-\frac{h^2 R_g^2}{3}\right] \tag{1}$$

Equation (1) applies to macromolecules in the limits of a dilute solution and small h values.

More detailed information of the molecular structure can be obtained from the distance distribution function p(r), which is related to the SAXS desmeared (free from geometrical collimation effects) intensity I(h) by:

$$p(r) = \frac{1}{2\pi^2} \int_0^\infty I(h)\,(hr)\sin(hr)\,dh \tag{2}$$

The p(r) function is proportional to the number of pair of electrons separated by the distance r which are encountered by combinations between all the elements of the macromolecule.

The radius of gyration of macromolecules in solution is usually determined by applying Eq. (1). It can also be determined starting from the distance distribution function p(r) with the advantage that, in this case, the whole scattering curve is used in the calculation and not only a small fraction as when Guinier approximation is used. The radius of gyration of the molecule is related to p(r) by:

$$R_g^2 = \frac{\int_0^\infty p(r)\,r^2\,dr}{2\int_0^\infty p(r)\,dr} \tag{3}$$

The distance distribution function, p(r), has been determined, for every pH, by indirect Fourier transformation using the ITP program developed by Glatter (1977). This method was shown to be more efficient than the direct Fourier transformation (Eq. (2)) for which termination and background effects are strong (Glatter 1982). This program was also used to determine the desmeared and smoothed scattered intensity I(h), free from smearing collimation effects.

The theoretical functions p(r) were calculated using the program Multibody (Glatter 1980), modified in order to make molecular model building easier (Olivieri 1992). The models used in this program were generated from an arrangement of small spheres which reproduce the desired molecular shape and size. The intensity of the X-ray scattering produced by each sphere with a radius R_s, I_s (h), is given by:

$$I_s(h) = \left[\frac{3\sin h R_s - h R_s \cos h R_s}{h^3 R_s^3}\right] \tag{4}$$

The program Multibody calculates the resulting function p(r) of the complete set of spheres for the proposed spatial distribution.

3. Results and discussion

The experimental scattering intensity functions, J(h), of HSA for infinite dilution are plotted in Fig. 2 for the different pH values. Guinier plots (log I(h) versus h^2) of the different desmeared scattering functions are displayed in Fig. 3. The slopes of the linear portions of these SAXS plots were determined to obtain the radius of gyration of HSA for different pH. The minimum value of R_g (26.1 Å) corresponds to pH 3.5 and the maximum (35.4 Å) to pH 2.5. For the other pH values the radii of gyration vary between 31 and 33 Å.

The radii of gyration of HSA inferred from the experimental SAXS results for different pH are displayed in Fig. 4. The discrepancy between the R_g values obtained using Eqs. (1) and (3) lies within the margin of experimental error. The results corresponding to pH 2.5 and 3.5 deserve special attention. At pH 2.5 the value of $R_g = 35.4$ Å suggests that the tertiary structure of the molecule is in an extended conformation in comparison to those corresponding to the other pH values. At pH 3.5, we found $R_g = 26.7$ Å which suggests the occurrence of an opposite effect, the molecule being in this case very compact. These changes in the radius of gyration indicate that HSA experiences distension and condensation when the pH is varied. This in turn implies significant differences in the configuration of subdomains of HSA as a function of pH.

Theoretical models were therefore proposed for the structure at any given pH. The theoretical distance distribution functions, p(r), were calculated for these models using the Multibody program and then compared with the experimental p(r) functions determined by using the ITP program from SAXS data.

The proposed models for albumin are composed of six *blocks* (or subdomains) which may adopt different spatial configurations for different pH. These six blocks were selected to represent the six subdomains of HSA shown in Fig. 5. The subdomains used in the models were built up of circular slices, each of them consisting of small spheres of 1 Å in diameter. This small value for the basic sphere diameter was chosen to remove any influence of its geometry in the calculated p(r) functions. These slices, with diameters between 18 and 30 Å were stacked to form oblate or prolate blocks (Olivieri 1992). The elaboration of the

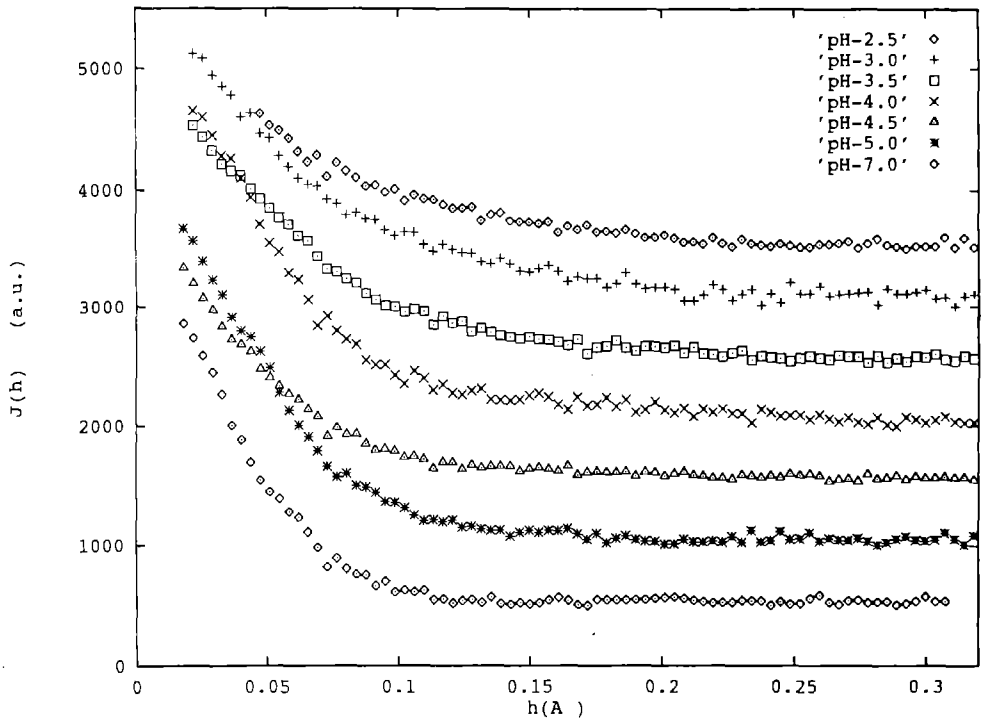

Fig. 2. Experimental small-angle X-ray scattering curves, J(h), after extrapolation to zero concentration in arbitrary units. The curves corresponding to different pH were vertically displaced for clarity

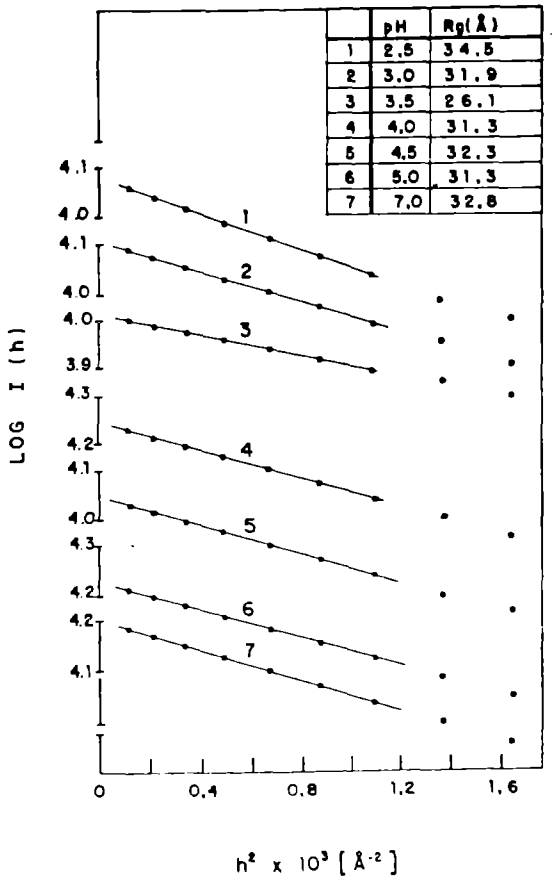

Fig. 3. Guinier plot of the SAXS intensities, I(h), for different pH after suppression of smearing effects. The straight lines were obtained by least-squares fitting in the region $h^2 < 1.09 \times 10^{-3}$ Å^{-2}. The radii of gyration of the macromolecule, calculated by Eq. (1), are given in the inset

different proposed models is compatible with the crystallographic structural model (He and Carter 1992) for HSA, in which changes in the arrangement of subdomains are possible, principally due to the absence of inter-domain disulphide bridges.

A number of molecular models of HSA at different pH were tested. The search was made by modifying the arrangement between subdomains, step by step, in such a way as to improve the overall agreement between theoretical and experimental p(r) functions. The process was stopped when, after a number of trials, no additional improvement was obtained.

The models that produced the best agreement between the theoretical and the experimental p(r) functions are shown in Fig. 5. In the same figure the distance distribution functions are presented for each pH. The theoretical p(r) functions determined from the proposed models exhibit most of the features of the experimental p(r) functions for every pH value.

A first peak in the experimental p(r) curves at a short distance (r ~ 20 Å) is apparent in Fig. 5a. It is related to spatial correlations of the scattering centres inside each of the 6 subdomains of HSA. The proposed models are made up of blocks which are located such that a peak r ~ 20 Å is apparent in the theoretical curves of p(r). By comparing several p(r) functions corresponding to different pH's, we observe that the first peak at 20 Å is less pronounced for pH > 2.5 because of the stronger overlapping effect of a second peak at a longer distance.

The second peak where 38 Å < r < 41 Å is associated with the correlations between different subdomains (the blocks in the theoretical model) (Fig. 5a). The variation of the position of the maximum indicates a change in the distances between first neighbour subdomains.

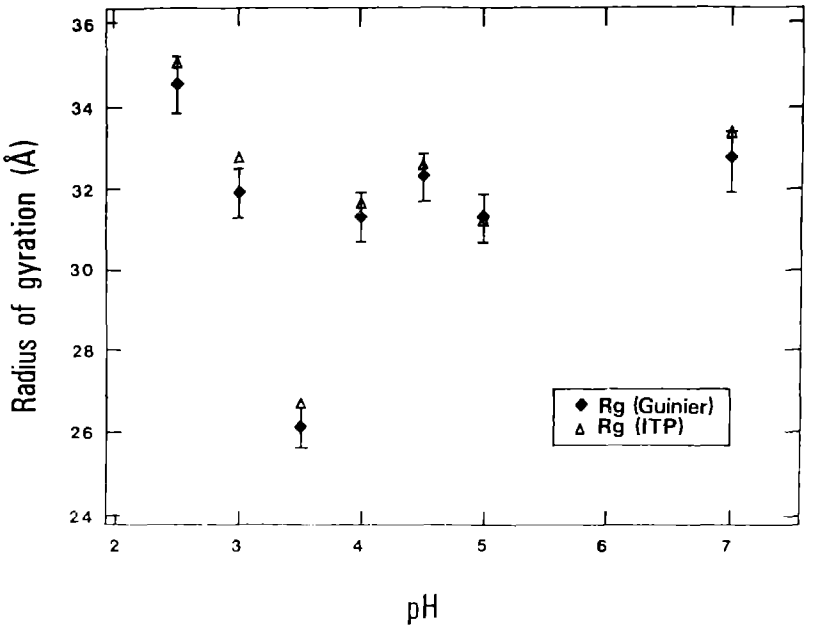

Fig. 4. Radii of gyration R_g (Guinier) and R_g (ITP) obtained from Eq. (1) and using the ITP program, respectively, as functions of pH. The agreement of both values of the radii of gyration (Guinier and ITP) indicates that no significant molecular aggregation occurs and, consequently, that the variation in R_g with pH is actually due to structural changes in the molecule

A third peak, which is apparent at pH values of 2.5, 3.5, 5.0 and 7.0, lies at r ~ 60 Å and is related to correlations between subdomains (or blocks) which belong to second or further nearest neighbours (Fig. 5 a, b, e, f). The pronounced extension and contraction of the molecule, when comparing the structures corresponding to different pH, can be deduced from the dislocation and/or disappearance of the third peak for certain pH values.

The changes in the arrangement of subdomains, as a response to changes in pH, is related to the existence and location of the disulphide bridges which permits the modification of the tertiary structure. The free electrical charges of domains I, II and III are −9e, −8e, and +2e, respectively at pH 7.0 (Peters 1985) is possibly one of the factors responsible for the different subdomain arrangement observed in HSA for different pH.

Our results indicate that at pH 2.5 (Fig. 5 a) the molecule exhibits an extended configuration (R_g = 34.5 Å) with a large accessible area; the maximum radius of each subdomain is of the order of 22 Å. This conclusion is consistent with Foster's results for form E (Foster 1977).

At pH 3.5 (Fig. 5 b), we observe that the radius of gyration, R_g = 26 Å, is significantly smaller than at pH 2.5. The subdomains I-A and I-B are in close contact appearing as a single block whereas the other domains have the same size and relative position as in the more extended configuration observed for pH 2.5. However, the correlation between the theoretical and experimental functions p(r), in the region 40 Å < r < 60 Å is relatively weak, and attempts to improve this correlation were unsuccessful. Other configurations, not considered in this work, may eventually provide a better agreement. At pH 3.6, BSA was suggested to exist as an elipsoid with a compact nucleus containing 66% of the protein and a radius of gyration of 27.2 Å (Luzzati et al. 1961). Porcine serum albumin (PSA) at pH 3.7 was shown by SAXS to exist as a flat prism with a radius of gyration of 38 Å (Laggner et al. 1971). This flat prism was modelled as consisting of two juxtaposed cylinders. The radii of gyration of HSA, this study, and BSA (Luzzati et al. 1961) at pH's 3.5 and 3.6, respectively, are in close agreement. However, the value obtained for PSA at pH 3.7 (Laggner et al. 1971) is greater. Another model for BSA also at pH 3.6 based on SAXS, intrinsic viscosities and diffusion coefficients results was proposed to consist of three spheres with radii 19, 26 and 19 Å arranged in a row (Bloomfield 1966).

Between pH 4.0 and 4.5 (Fig. 5 c, d), close to the isoelectric point (pH ~ 4.8), the molecule adopts a compact configuration with R_g values ranging between 31.6 and 32.6 Å. The subdomains are relatively closer to each other and the central region of the molecule is less accessible in comparison to the model at pH 2.5. However, at this pH, the size of subdomains I-A, II-A and III-A increases to approximately 30 Å whereas the size of subdomains I-B, II-B and III-B experiences a smaller increase to about 24 Å. A change in pH from 4.0 to 4.5 results in a minor rearrangement of the subdomain II-A with no significant change in the diameters of the subdomains. A radius of gyration of 29.8 Å was obtained in a previous investigation for BSA at pH 4.6 for which two models were proposed: i) a right prism with dimensions 106 × 21.5 × 50 Å and ii) a rectangular parallelepiped with dimensions 82.5 × 27.5 × 63 Å. (Anderegg et al. 1955). However, the authors were unable to decide between the two proposed models (Anderegg et al. 1955).

At pH 5.0, above the isoelectric point, domain I is rotated by approximately 90° from the configuration at pH 4.0 and 4.5 (Fig. 5 e). The molecule is roughly heart shaped with a radius of gyration of 31.3 Å, and the relative orientations and sizes of the individual subdomains are the same as at pH 4.0 and 4.5. Our model of HSA at this pH possesses the same shape as HSA found in the crystalline state (Carter et al. 1990). For PSA at pH 5.1 a prolate ellipsoid with axial ratios of 0.66:1:2, and a radius of

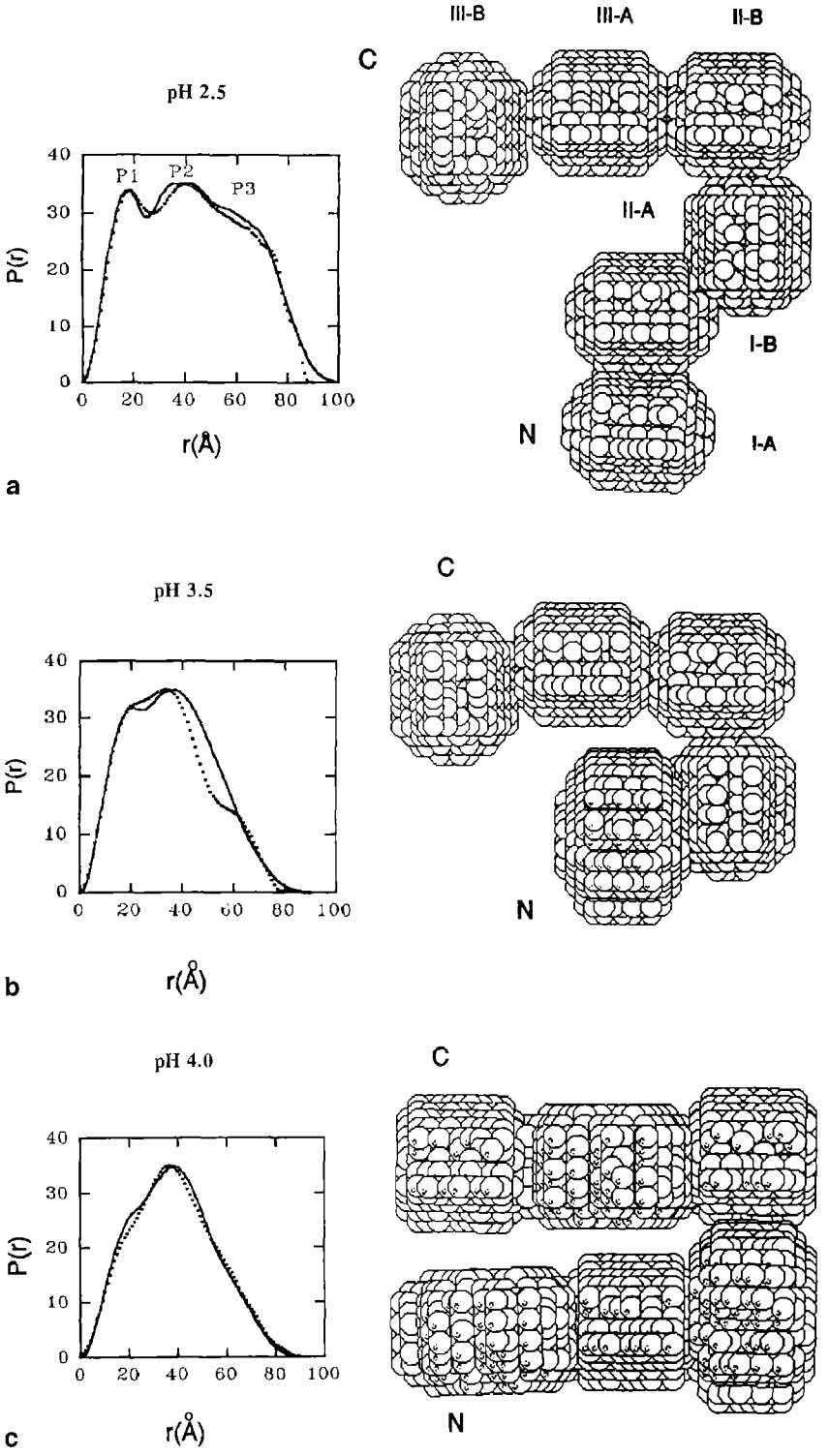

Fig. 5 a–f. Proposed structural models and the corresponding theoretical (continuous line) and experimental (dotted line) distance distribution functions, p(r), for human serum albumin. **a** Exhibits the proposed model at pH 2.5; N and C indicate the amino and carboxyl terminii, respectively; labels are given for each subdomain; the positions of the three peaks discussed in the text (P_1, P_2 and P_3) are indicated. The structural models and the associated p(r) functions at other pH values are displayed in **b**, **c**, **d**, **e** and **f**

gyration of 32 Å was proposed (Laggner et al. 1971). At pH 5.3, BSA was shown to exist as an ellipsoid of revolution (Luzzati et al. 1971), with a radius of gyration of 30.6 Å, but the authors could not distinguish between an elongated or prolate ellipsoid. SANS of a solution at pH 5.1 also indicated that BSA exists as a prolate ellipsoid with a radius of gyration of 30.5 Å (Bendedouch and Chen 1983).

At pH 7.0 (Fig. 5 f) the molecule exhibits a rather extended configuration and possesses a radius of gyration of 33.4 Å. The relative positions of subdomains I-A and I-B change and I-B is more distant from III-A when compared to the structure at pH 5.0. Again, the arrangement of domains II and III does not experience changes and the size of the subdomains is the same as at pH 5.0. These results are consistent with the structure determined crystallo-

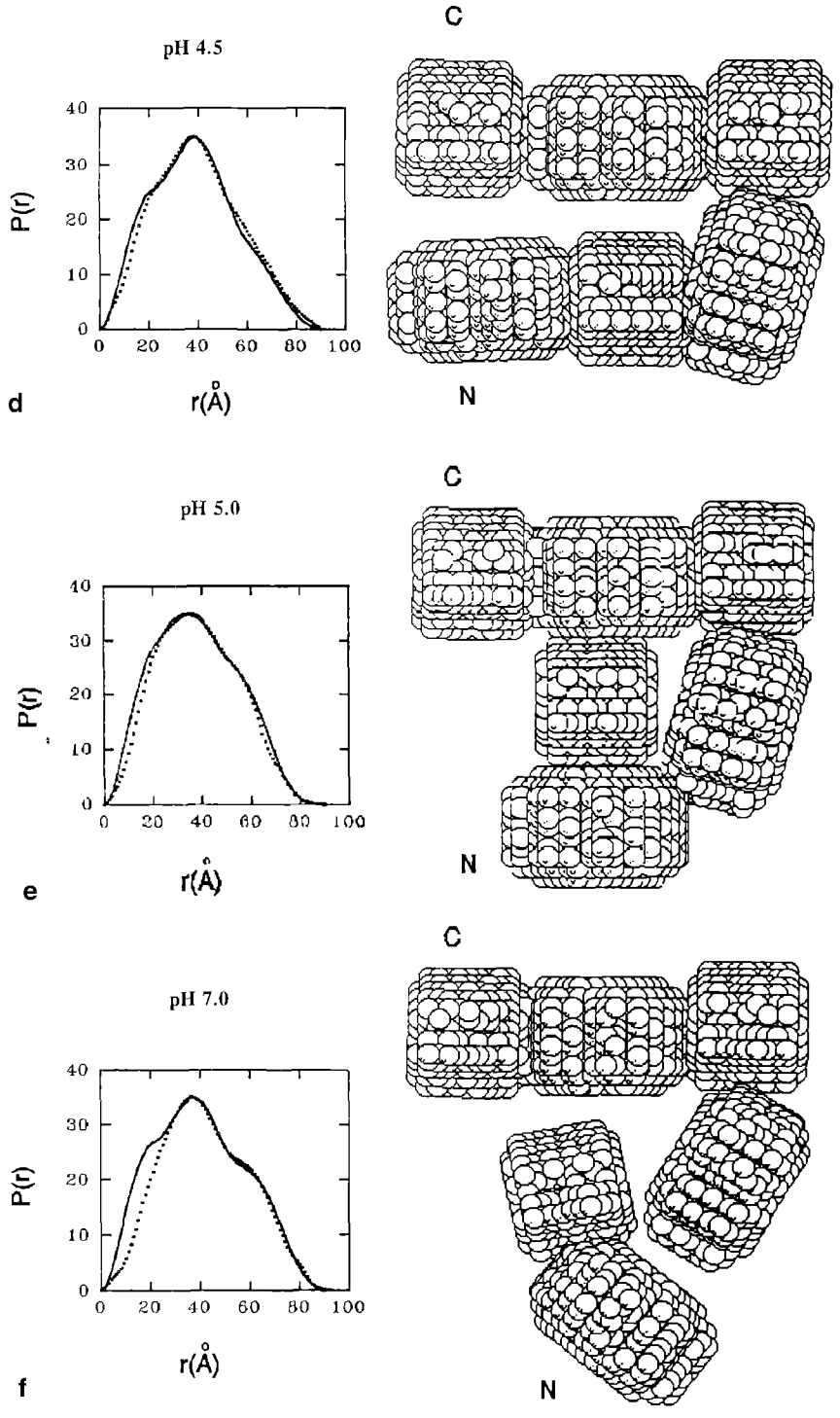

Fig. 5d–f.

graphically for HSA (Carter et al. 1990) and for Horse Serum Albumin (Ho et al. 1993), which suggests that the structure of albumin between pH 5.5 and 7.0 can be approximated by an equilateral triangle with length of the sides of 80 Å and a thickness of 30 Å.

We used the same basic structure of the macromolecule in the crystalline state, determined for pH 5–7, as starting point for all the structural models of subdomains corresponding to different pH in the range 2.5–7.0. We implicitly assumed that the structures corresponding to all pH consist of different arrangements of essentially the same subdomains. On the other hand, the helical content of albumin in the crystalline structure, estimated to be 67% (He and Carter 1992), being greater than found under any other pH, indicates the existence of structural differences within the subdomains for pH < 5. Nevertheless, the agreement found between the experimental and the theoretical p(r) functions for all pH suggests that internal differences do

not modify the overall subdomain structures. This indicates that, even for very acidic pH, for which the helix content is reduced, the existence of adjacent disulphide bridges contributes to the stabilization of the overall subdomain structure preserving their globular shape.

4. Conclusion

The present SAXS study proposes different structural models for HSA in solution under a wide pH range and indicates the existence of different arrangements of molecular domains and subdomains for different pH conditions.

Our SAXS results are consistent with those of other authors obtained at specific pH's for serum albumin from different sources, which display a high degree of homology. The models suggested earlier correspond to single pH values and do not provide information on correlations and systematic differences in subdomain arrangements induced in serum albumin by changes in pH. Our SAXS results indicate that the individual subdomains behave as nearly invariant units, the weak links between subdomains allowing for significant rearrangements of subdomains in response to changes in pH. The HSA molecule varies in shape between an extended subdomain configuration at low pH (2.5) and a roughly triangular domain configuration for pH ranging from 5 to 7. The latter structure is similar to that observed in the crystalline state (He and Carter 1992).

Although SAXS is a low resolution technique which does not provide information on details of the macromolecular structure such as atomic parameters, rotations of nearly isodiametric subdomains and degree of helicity, this study demonstrates that SAXS is indeed sensitive of modifications in molecular configuration of HSA.

This systematic study of HSA molecular subdomain configuration as a response to changes in pH, within a wide pH range (2.5–7.0), may help to explain some of the properties of this molecule and its involvement in numerous biological processes.

Acknowledgement. We gratefully acknowledge FAPESP and CNPq (Brazil) for financial support. We thank Y. P. Mascarenhas and H. Chaimovich for discussions and R. K. Arni for comments and critical reading of the manuscript.

References

Anderegg JW, Beeman WW, Shulman S, Kaesberg P (1955). An Investigation of the Size, Shape and Hydration of Serum albumin by Small-Angle X-Ray Scattering. J Am Chem Soc 77:2927

Behens GH, Spiekerman AM, Brown JR, (1975) Structure of human serum albumin. Fed Proc 34:591

Bendedouch D, Chen SH (1983) Structure and interparticle, interactions of bovine serum albumin in solution studies by Small Angle Neutron Scattering. J Phys Chem 87:1473–1477

Bloomfield V (1966) The Structures of Bovine Serum Albumin at Low pH. Biochemistry 5:684–689

Brown JR (1977) Serum albumin: amino acid sequence. In Albumin Structure, Functions and Uses. Rosenoer VM, Oratz M, Rothschild MA (eds) Pergamon Press, Oxford, pp 27–51

Carter DC, He XM (1990) Structure of human serum albumin. Science 249:302–303

Carter DC, He XM, Munsons H, Twigg RD, Gernert KM, Broom MB, Miller TK (1989) Three-dimensional structure of human serum albumin. Science 244:1195–1198

Foster JF (1977) Albumin structure, function and uses. Rosenoer VM, Oratz M, Rothschild MA (eds) Pergamon Press, Oxford, pp 53–84

Glatter O (1977) J Appl Cryst 10:415–421

Glatter O (1980) Acta Phys Aust 52:243–256

Glatter O (1982) Small Angle X-Ray Scattering Glatter O, Kratky O (eds) Academic Press, London

Guinier A, Fournet G (1955) Small-Angle Scattering of X-rays. J. Wiley and Sons, New York

He XM, Carter DC (1992) Atomic structure and chemistry of human serum albumin. Nature 358 (6383):209–215

Ho JX, Holowachuk EW, Norton EJ, Twigg PD, Carter DC (1993) X-ray and primary structure of horse serum albumin (Equus Caballus) at 0.27 nm Resolution. Eur J Biochem 215:205–212

Kragh-Hanse (1981) Molecular aspects of ligand binding to serum albumin. Pharmacol Rev 33:17–52

Kratky O (1982) Small Angle X-Ray Scattering. Glatter O, Kratky O (eds) Academic Press, London

Laggner P, Kratky O, Palm WH, Holasek A (1971) Mh Chem 102:1729

Luzzati V, Witz J, Nicolaieff A (1961) La structure de la serum albumine de boeuf en solution a pH 5,3 et 3,6: Etude par diffusion centrale absolue des rayons X. J Mol Biol 3:379–392

MacLachlan AD, Walker JE (1977) Evolution of serum albumin. J Mol Biol 112:543–558

Meloun B, Moravek L, Kostra V (1975) Complete amino acid sequence of human serum albumin. FEBS Lett 58:134–137

Olivieri JR (1992) PhD Thesis, University of São Paulo, Brazil

Peters T Jr (1985) Adv Protein Chem 37:161

Squire PG, Moser P, O'Konski CT (1968) The hydrodynamic properties of bovine serum albumin, monomer and dimer. Biochemistry 7 (12):4261–4272